

ATOMIC AND MOLECULAR PHYSICS

## Determination of the transport properties in 4H-SiC wafers by Raman scattering measurement<sup>\*</sup>

To cite this article: Sun Guo-Sheng *et al* 2011 *Chinese Phys. B* **20** 033301

View the [article online](#) for updates and enhancements.

### You may also like

- [Infrared reflectance study of 3C-SiC epilayers grown on silicon substrates](#)  
Lin Dong, Guosheng Sun, Liu Zheng *et al.*
- [Homojunction structure amorphous oxide thin film transistors with ultra-high mobility](#)  
Rongkai Lu, Siqin Li, Jianguo Lu *et al.*
- [Carrier lifetime and breakdown phenomena in SiC power device material](#)  
T Kimoto, H Niwa, T Okuda *et al.*

# Determination of the transport properties in 4H-SiC wafers by Raman scattering measurement\*

Sun Guo-Sheng(孙国胜)<sup>a)b)c)†</sup>, Liu Xing-Fang(刘兴昉)<sup>b)</sup>, Wu Hai-Lei(吴海雷)<sup>b)</sup>,  
 Yan Guo-Guo(闫果果)<sup>b)</sup>, Dong Lin(董林)<sup>b)</sup>, Zheng Liu(郑柳)<sup>b)</sup>,  
 Zhao Wan-Shun(赵万顺)<sup>b)</sup>, Wang Lei(王雷)<sup>b)</sup>, Zeng Yi-Ping(曾一平)<sup>a)b)</sup>,  
 Li Xi-Guang(李锡光)<sup>c)</sup>, and Wang Zhan-Guo(王占国)<sup>a)</sup>

<sup>a)</sup>Key Laboratory of Semiconductor Material Sciences, Institute of Semiconductors,  
 Chinese Academy of Sciences, Beijing 100083, China

<sup>b)</sup>Material Science Center, Institute of Semiconductors, Chinese Academy of Sciences, Beijing 100083, China

<sup>c)</sup>Dongguan Tianyu Semiconductor, Inc., Dongguan 523000, China

(Received 29 September 2010; revised manuscript received 29 November 2010)

The free carrier density and mobility in n-type 4H-SiC substrates and epilayers were determined by accurately analysing the frequency shift and the full-shape of the longitudinal optic phonon–plasmon coupled (LOPC) modes, and compared with those determined by Hall-effect measurement and that provided by the vendors. The transport properties of thick and thin 4H-SiC epilayers grown in both vertical and horizontal reactors were also studied. The free carrier density ranges between  $2 \times 10^{18} \text{ cm}^{-3}$  and  $8 \times 10^{18} \text{ cm}^{-3}$  with a carrier mobility of  $30\text{--}55 \text{ cm}^2/(\text{V}\cdot\text{s})$  for n-type 4H-SiC substrates and  $1 \times 10^{16}\text{--}3 \times 10^{16} \text{ cm}^{-3}$  with mobility of  $290\text{--}490 \text{ cm}^2/(\text{V}\cdot\text{s})$  for both thick and thin 4H-SiC epilayers grown in a horizontal reactor, while thick 4H-SiC epilayers grown in vertical reactor have a slightly higher carrier concentration of around  $8.1 \times 10^{16} \text{ cm}^{-3}$  with mobility of  $380 \text{ cm}^2/(\text{V}\cdot\text{s})$ . It was shown that Raman spectroscopy is a potential technique for determining the transport properties of 4H-SiC wafers with the advantage of being able to probe very small volumes and also being non-destructive. This is especially useful for future mass production of 4H-SiC epi-wafers.

**Keywords:** 4H-SiC, Raman scattering, LOPC modes, transport properties

**PACS:** 33.20.Fb, 71.20.Nr

**DOI:** 10.1088/1674-1056/20/3/033301

## 1. Introduction

Over the last few years, silicon carbide (SiC) power devices have developed very rapidly and some of them, such as Schottky Barrier Diodes (SBDs) and MESFETs, are well established on the market. With the unique properties of the 4H-SiC polytype, 4H-SiC power devices with a voltage-blocking capability greater than 10 kV have been demonstrated, which include PiN,<sup>[1]</sup> Junction Barrier Schottky (JBS),<sup>[2]</sup> DMOSFET,<sup>[3]</sup> IGBT,<sup>[4,5]</sup> GTO<sup>[6]</sup> etc. The requirement of a cost-effective, reproducible and reliable epitaxial process has led to the introduction of multi-wafer systems.<sup>[7,8]</sup> Very thick epilayers ( $> 100 \mu\text{m}$ ) for  $> 10 \text{ kV}$  devices require a fast epitaxial growth of 4H-SiC, with higher growth rates being effective in enhancing the reactor throughput. *in-situ* doping in 4H-SiC is another topic of strong interest and many studies of doped 4H-SiC have been made.<sup>[9]</sup>

Usually, electrical characterization is performed by Hall-effect and  $C\text{--}V$  measurements.<sup>[9]</sup> These procedures need electric contacts and give information on the transport properties averaged over relatively large sample volumes. It has been shown that Raman spectroscopy is a powerful technique for studying the transport properties in SiC semiconductors,<sup>[10–12]</sup> the characterization of ion-implanted SiC in order to evaluate the amount of damage, the dose of implanted atoms, their electrical activity and the recovery of crystallinity during post-annealing, and even the characterization of defects in SiC. The main advantages of employing Raman spectroscopy are the small local noninvasive probes used and that no special preparation is required for the mass-production of SiC epi-wafers. Raman scattering from LO-phonon–plasmon–coupled (LOPC) modes was previously used to study III–V semiconductors, which have high carrier mobil-

\*Project supported by the National Natural Science Foundation of China (Grant No. 60876003) and the Knowledge Innovation Project of Chinese Academy of Sciences (Grant Nos. Y072011000 and ISCAS2008T04) and the Science and Technology Projects of the State Grid Corporation of China (ZL71-09-001).

†Corresponding author. E-mail: gshsun@red.semi.ac.cn

© 2011 Chinese Physical Society and IOP Publishing Ltd

<http://www.iop.org/journals/cpb> <http://cpb.iphy.ac.cn>

ities and later applied to materials with relatively low carrier mobilities such as GaP, ZnO, ZnSe and SiC.<sup>[11]</sup> Recent rapid progress in the epitaxial growth of good quality 4H-SiC has motivated us to study their transport properties systematically using Raman scattering measurements.

In the present work, we have observed the coupled LOPC modes with backscattering geometry from the (0001) plane and have analysed the line shapes of the coupled modes by fitting the theoretical band shape, taking the plasmon frequency, carrier- and phonon-damping rates as adjustable parameters. From the analysis, the carrier concentration and mobilities in both the n<sup>+</sup> 4H-SiC substrates and the 4H-SiC homoepitaxial layers were obtained and compared with that obtained by Hall-effect and C-V measurements and that provided by the manufacturers. It was shown that Raman scattering can be used to determine transport properties in 4H-SiC wafers.

## 2. Experiment

Three different kinds of 4H-SiC wafers were studied in this work. The first are two heavily nitrogen doped n<sup>+</sup> 4H-SiC substrates purchased from two vendors (A and B), which were named No. 1(A) and No. 2(B). The second are two unintentionally doped thick 4H-SiC homoepitaxial layers (for the fabrication of power devices) with a thickness of 32 and 20 μm grown on n<sup>+</sup> 4H-SiC substrates in horizontal and vertical low temperature chemical vapour deposition (LPCVD) reactors, respectively, in the authors' group, which were named No. 3 and No. 4. The third are three lightly doped n-type 4H-SiC homoepitaxial layers with a thickness of about 1-2 μm, which were named E04013, A04012, and D04011, respectively, and were used as channel layers in MESFETs.

Raman-scattering measurements were carried out at room temperature using 488 nm line of an Ar ion laser for excitation and a charge-coupled detector (CCD) was used to detect the scattered signals. The near backscattering configuration perpendicular to the (0001) face of 4H-SiC wafers was taken as collection geometry. The excitation spot onto the sample surface was in the order of a micrometer in size.

## 3. Theoretical analysis of LOPC intensity

The Raman intensity of the coupled mode for 4H-SiC can be written as the following expression

by assuming a dominant deformation potential, DP, mechanism<sup>[10,13]</sup>

$$I(\omega) = SA(\omega) \operatorname{Im} \left( -\frac{1}{\varepsilon(\omega)} \right), \quad (1)$$

where  $\omega$  is the Raman frequency,  $S$  is a proportionality constant,  $\varepsilon(\omega)$  is the dielectric function, and  $A(\omega)$  is given by the following expression:<sup>[12,14]</sup>

$$\begin{aligned} A(\omega) = & 1 + 2C \frac{\omega_T^2}{\Delta} [\omega_P^2 \gamma_P (\omega_T^2 - \omega^2) \\ & - \omega^2 \Gamma (\omega^2 + \gamma_P^2 - \omega_P^2)] \\ & + \frac{C^2 \omega_T^4}{\Delta (\omega_L^2 - \omega_T^2)} \{ \omega_P^2 [\gamma_P (\omega_L^2 - \omega_T^2) \\ & + \Gamma (\omega_P^2 - 2\omega^2)] + \omega^2 \Gamma (\omega^2 + \gamma_P^2) \}, \quad (2) \\ \Delta = & \omega_P^2 \gamma_P [(\omega_T^2 - \omega^2)^2 + \omega^2 \Gamma^2] \\ & + \omega^2 \Gamma (\omega_L^2 - \omega_T^2) (\omega^2 + \gamma_P^2), \quad (3) \end{aligned}$$

where  $\omega_T$  and  $\omega_L$  are the frequencies of TO and LO phonons, respectively,  $\omega_P$  is the plasmon frequency,  $\gamma_P$  is the plasmon damping constant,  $\Gamma$  is the phonon damping constant, and  $C$  is the Faust-Henry coefficient,<sup>[15]</sup> which is related to the Raman-intensity ratio of LO- and TO-phonon bands in undoped crystals.<sup>[16]</sup> The dielectric function  $\varepsilon(\omega)$  is given by a sum of the contributions from both phonons and plasmons as follows

$$\varepsilon(\omega) = \varepsilon_\infty \left( 1 + \frac{\omega_L^2 - \omega_T^2}{\omega_T^2 - \omega^2 - i\omega\Gamma} - \frac{\omega_P^2}{\omega(\omega + i\gamma_P)} \right), \quad (4)$$

where  $\varepsilon_\infty$  is the high frequency dielectric constant. The plasma frequency  $\omega_P$  is given by the following expression:

$$\omega_P = \sqrt{\frac{4\pi n e^2}{\varepsilon_\infty m^*}}, \quad (5)$$

where  $n$  is the free carrier concentration,  $m^*$  is the electron effective mass, and  $e$  is the electronic charge.

The plasmon damping constant,  $\gamma_P$ , is expressed as a function of the carrier mobility,  $\mu$ , by the following equation:

$$\gamma_P = \frac{e}{m^* \mu}. \quad (6)$$

It can be seen clearly from Eqs. (5) and (6) that both free carrier concentration,  $n$ , and mobility,  $\mu$ , can be calculated from the  $\omega_P$  and  $\gamma_P$  data obtained from the fit to Eq. (1) by taking  $\omega_P$  and  $\gamma_P$  as the adjustable parameters.

From Eq. (4), we obtained the following equation for dielectric function

$$\varepsilon(\omega) = \varepsilon_\infty \left( \frac{(\gamma_P \omega^2 \Gamma + \omega_L^2 \omega^2 - \omega^4 - \omega_P^2 \omega_T^2 + \omega_P^2 \omega^2) + i(\gamma_P \omega_L^2 \omega + \Gamma \omega_P^2 \omega - \Gamma \omega^3 - \gamma_P \omega^3)}{(\omega_T^2 \omega^2 - \omega^4 + \gamma_P \Gamma \omega^2) + i(\gamma_P \omega_T^2 \omega - \gamma_P \omega^3 - \Gamma \omega^3)} \right). \quad (7)$$

Then, the dielectric function can be rewritten as

$$\varepsilon(\omega) = \varepsilon_\infty \frac{\Pi + i\Lambda}{M + iN}, \quad (8)$$

where

$$\begin{aligned} \Pi &= \gamma_P \omega^2 \Gamma + \omega_L^2 \omega^2 - \omega^4 - \omega_P^2 \omega_T^2 + \omega_P^2 \omega^2, \\ \Lambda &= \gamma_P \omega_L^2 \omega + \Gamma \omega_P^2 \omega - \Gamma \omega^3 - \gamma_P \omega^3, \\ M &= \omega_T^2 \omega^2 - \omega^4 + \gamma_P \Gamma \omega^2, \\ N &= \gamma_P \omega_T^2 \omega - \gamma_P \omega^3 - \Gamma \omega^3. \end{aligned}$$

The reciprocal of the dielectric function and its imaginary part can be obtained as following equations.

$$\frac{1}{\varepsilon(\omega)} = \frac{1}{\varepsilon_\infty} \frac{(M\Pi + N\Lambda) + i(N\Pi - M\Lambda)}{\Pi^2 + \Lambda^2}, \quad (9)$$

$$\text{Im} \left[ -\frac{1}{\varepsilon(\omega)} \right] = -\frac{1}{\varepsilon_\infty} \frac{N\Pi - M\Lambda}{\Pi^2 + \Lambda^2}. \quad (10)$$

From Eq. (2)  $A(\omega)$  can be rewritten as following expression:

$$A(\omega) = 1 + 2AC \frac{\omega_T^2}{\Delta} + \frac{BC^2 \omega_T^4}{\Delta(\omega_L^2 - \omega_T^2)}, \quad (11)$$

where

$$\begin{aligned} A &= \omega_P^2 \gamma_P (\omega_T^2 - \omega^2) - \omega^2 \Gamma (\omega^2 + \gamma_P^2 - \omega_P^2), \\ B &= \omega_P^2 [\gamma_P (\omega_L^2 - \omega_T^2) + \Gamma (\omega_P^2 - 2\omega^2)] \\ &\quad + \omega^2 \Gamma (\omega^2 + \gamma_P^2), \\ \Delta &= \omega_P^2 \gamma_P [(\omega_T^2 - \omega^2)^2 + \omega^2 \Gamma^2] \\ &\quad + \omega^2 \Gamma (\omega_L^2 - \omega_T^2) (\omega^2 + \gamma_P^2). \end{aligned} \quad (12)$$

Therefore, the intensity of the LOPC profile in 4H-SiC,  $I(\omega)$ , can be deduced by following equation:

$$\begin{aligned} I(\omega) &= -\frac{S}{\varepsilon_\infty} \left( 1 + 2AC \frac{\omega_T^2}{\Delta} + \frac{BC^2 \omega_T^4}{\Delta(\omega_L^2 - \omega_T^2)} \right) \\ &\quad \times \frac{N\Pi - M\Lambda}{\Pi^2 + \Lambda^2}. \end{aligned} \quad (13)$$

Equation (13) is our final theoretical expression of the intensity of the LOPC profile used in our fitting procedure. Much attention should be paid to the values of several constants appearing in Eq. (13). For example, the proportionality constant,  $S$ , is independent of the carrier concentration according to Ref. [11]. Therefore,  $S$  was not used as the adjustable parameter for 4H-SiC wafers with different carrier concentrations. In this work, the coupled LOPC modes were fitted to Eq. (13) using  $\omega_P$ ,  $\gamma_P$  and  $\Gamma$  as the adjustable parameters, while others were kept as constants in our fitting procedure.

## 4. Results and discussion

Figure 1 shows typical Raman spectra for four different 4H-SiC wafers. No. 1 is an  $n^+$  substrate from vendor A and No.2 from vendor B. No. 3 and No. 4 are two thick unintentionally doped 4H-SiC homoepitaxial layers with thicknesses of 32 and 20  $\mu\text{m}$  grown on  $n^+$  substrates in horizontal and vertical LPCVD chambers, respectively, by the authors' group. According to the group-theoretical analysis and Raman selection rules for 4H-SiC polytypes, phonon bands with  $A_{1L}$  symmetry ( $A_{1L}$  for LO phonon) and  $E_2$  symmetry ( $E_{2T}$  for TO phonon) are allowed in backscattering geometry. The  $A_{1L}$  band peaks of wafers No. 4, No. 3, No. 2 and No. 1 located at 963.5, 965.2, 982.0 and 1005  $\text{cm}^{-1}$ , respectively. It can be seen clearly that  $A_{1L}$  band shifts to the high frequency side and broadens, while the intensity decreases from wafer No. 4 to No. 1. These profiles show typical features of LOPC mode in 4H-SiC. On the other hand, the TO phonon bands located at 776.4  $\text{cm}^{-1}$  ( $E_{2T}$ ) are sharp and almost the same within  $\pm 1 \text{ cm}^{-1}$  for these four different wafers. These TO-phonon peak positions agree well with the published data.<sup>[17–19]</sup>

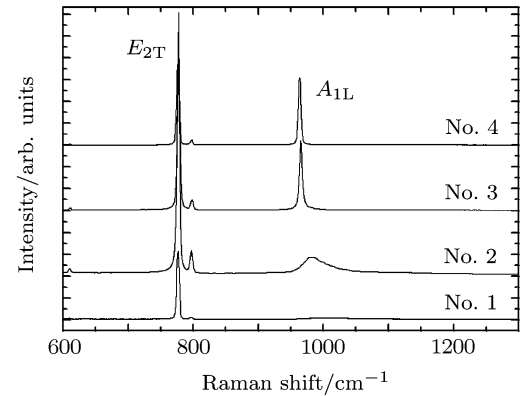


**Fig. 1.** Raman spectra for four different 4H-SiC wafers. No. 1 and No. 2 are two  $n^+$  substrate from different manufacturers. No. 3 and No. 4 are two thick 4H-SiC homoepitaxial layers with thicknesses of 32 and 20  $\mu\text{m}$  grown in horizontal and vertical LPCVD chambers, respectively, by the authors' group.

Figure 2 shows experimental (black dots) and calculated (solid line) band shapes of the LOPC modes for four 4H-SiC wafers named as (a) No. 1 (substrate from vendor A), (b) No. 2 (substrate from vendor

B), (c) No. 3 (thick epilayer 1), and (d) No. 4 (thick epilayer 2) as shown in Fig. 1. The solid lines correspond to fits to Eq. (13). The intensity of the LOPC mode has been normalized by the TO-phonon peak intensity ( $E_{2T}$ ). Our analysis is based on the method suggested by Irmer *et al.*<sup>[14]</sup> and Chafai *et al.*<sup>[10]</sup> ascribing to electro-optical and deformation potential as dominant mechanisms for Raman scattering. From the fit parameters,  $\omega_p$  and  $\gamma_p$  the carrier concentration ( $n$ ) and carrier mobility ( $\mu$ ) are obtained using Eqs. (5) and (6), respectively, as shown in Table 1. The carrier concentration for No. 1 4H-SiC substrate wafer is  $7.5 \times 10^{18} \text{ cm}^{-3}$  with the carrier mobility of  $32 \text{ cm}^2/(\text{V}\cdot\text{s})$ , while that for No. 4 thick 4H-SiC epilayer is  $1.60 \times 10^{16} \text{ cm}^{-3}$  with a mobility of around

$492 \text{ cm}^2/(\text{V}\cdot\text{s})$ . These data are very close to that provided by vendor A ( $5.0 \times 10^{18} \text{ cm}^{-3}$ ) and that reported in previous work,<sup>[20]</sup> respectively. The calculated carrier concentration for No. 2 4H-SiC substrate wafer is  $2.45 \times 10^{18} \text{ cm}^{-3}$  with the carrier mobility of  $53 \text{ cm}^2/(\text{V}\cdot\text{s})$ . It can be seen that the transport properties of No. 2 wafer are slightly different from No. 1. The carrier concentration of No. 3 wafer is  $8.10 \times 10^{16} \text{ cm}^{-3}$  with a mobility of  $380 \text{ cm}^2/(\text{V}\cdot\text{s})$ , which is in agreement with the  $C$ - $V$  measurements by the authors' group. Compared with No. 4, the reason of higher carrier concentration for No. 3 wafer is that it was grown in a vertical reactor with much higher growth rate.

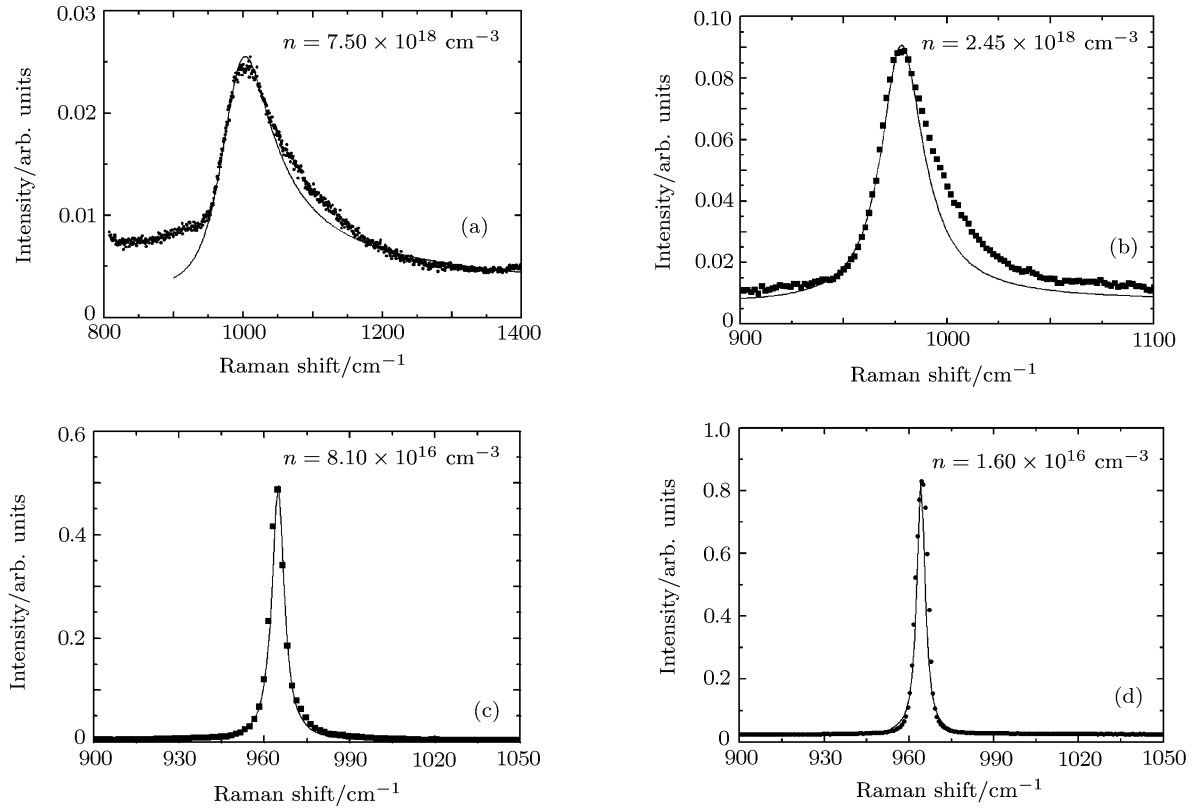
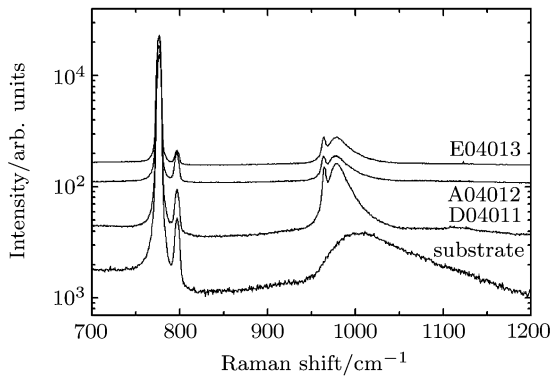


**Fig. 2.** Experimental (black dots) and calculated (solid line) band shapes of the LOPC modes for four 4H-SiC wafers named as (a) No. 1, (b) No. 2, (c) No. 3, and (d) No. 4 as shown in Fig. 1. The solid lines correspond to fits to Eq. (13).

**Table 1.** The calculated carrier concentration and mobility in four 4H-SiC wafers.

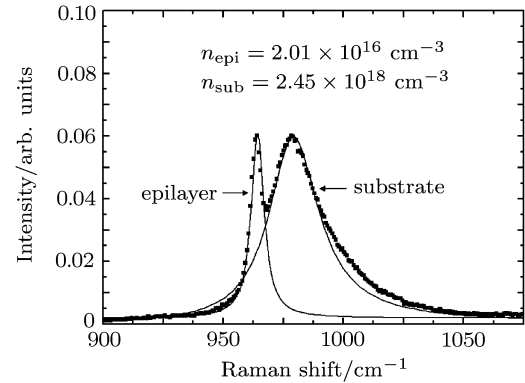
wafer No.	No. 1	No. 2	No. 3	No. 4
$n/\text{cm}^{-3}$	$7.5 \times 10^{18}$	$2.45 \times 10^{18}$	$8.10 \times 10^{16}$	$1.60 \times 10^{16}$
$\mu/(\text{cm}^2/(\text{V}\cdot\text{s}))$	32	53	380	492

Figure 3 shows the Raman spectra for three thin lightly doped n-type 4H-SiC epilayers (1–2  $\mu\text{m}$ ) grown on  $n^+$  4H-SiC substrate in a horizontal LPCVD chamber. For comparison, the Raman spectrum for the substrate on which the epilayer was grown is also shown in the figure. We know that the penetration depth of the 488 nm laser light is less than ten microns. As the thickness of the three thin 4H-SiC epilayers is about 1–2  $\mu\text{m}$ , the Raman spectra should contain information from the  $n^+$  4H-SiC substrate. By analysing these two peaks separately, the electrical properties of the epilayer can be obtained.



**Fig. 3.** The Raman spectra for three thin lightly doped n-type 4H-SiC epilayers (1–2  $\mu\text{m}$ ) grown on  $n^+$  4H-SiC substrate in a horizontal LPCVD chamber and the substrate used.

Figure 4 shows the typical experimental (black dots) and calculated (solid line) band shapes of the LOPC mode with two peaks for wafer E04013. The calculated carrier concentration is  $2.01 \times 10^{16} \text{ cm}^{-3}$  with a carrier mobility of  $431 \text{ cm}^2/(\text{V}\cdot\text{s})$  for the epilayer and  $2.45 \times 10^{18} \text{ cm}^{-3}$  with a mobility of  $54 \text{ cm}^2/(\text{V}\cdot\text{s})$  for the substrate. The electrical property of the thin epilayer is very close to that of No. 4 wafer as shown in Fig. 2. The carrier concentration of the substrate is 3 times less than that of No. 1 substrate wafer. This may be due to some unknown effects of the epilayer when the Raman signal comes out from the substrate.



**Fig. 4.** Experimental (black dots) and calculated (solid line) band shapes of the LOPC mode for wafer E04013. The solid lines correspond to fits to Eq. (13) for the two peaks originated from the epilayer and the substrate, respectively.

## 5. Conclusion

We have obtained the LOPC modes in 4H-SiC wafers. The free carrier density and mobility in n-type 4H-SiC substrates and epilayers were determined by accurately analysing the LOPC modes. The transport properties were also studied in thick and thin 4H-SiC epilayers grown in vertical and horizontal reactors. The free carrier density ranges between  $2 \times 10^{18} \text{ cm}^{-3}$  and  $8 \times 10^{18} \text{ cm}^{-3}$  with carrier mobility of  $30\text{--}55 \text{ cm}^2/(\text{V}\cdot\text{s})$  for n-type 4H-SiC substrates and  $1\text{--}3 \times 10^{16} \text{ cm}^{-3}$  with mobility of  $400\text{--}490 \text{ cm}^2/(\text{V}\cdot\text{s})$  for both thick and thin 4H-SiC epilayers grown in horizontal reactor. The thick 4H-SiC epilayer grown in a vertical reactor with much higher growth rate has a little higher carrier concentration of around  $8.1 \times 10^{16} \text{ cm}^{-3}$  with mobility of  $380 \text{ cm}^2/(\text{V}\cdot\text{s})$ . It is demonstrated that Raman scattering measurement is a potential technique for determining the transport properties in 4H-SiC wafers with the advantage of probing very small volumes and being non-destructive. This is especially useful for future mass production of 4H-SiC epi-wafers.

## Acknowledgement

The authors would like to thank Dr. Liu Yu-long at the Institute of Physics Chinese Academy of Sciences for his assistance with the Raman measurements.

## References

- [1] Hull B A, Sumakeris J J, Das M K, Richmond J T and Palmour J 2007 *Mater. Sci. Forum* **556–557** 895
- [2] Hull B A, Sumakeris J J, O’Loughlin M J, Zhang Q C, Richmond J, Powell A, Paisley M, Tsvetkov V, Hefner A and Rivera A 2009 *Mater. Sci. Forum* **600–603** 931

- [3] Ryu S H, Fatima H, Haney S, Zhang Q C, Stahlbush R and Agarwal A 2009 *Mater. Sci. Forum* **600–603** 1127
- [4] Zhang Q C, Jonas C, Sumakeris J, Agarwal A and Palmour J 2009 *Mater. Sci. Forum* **600–603** 1187
- [5] Das M K, Zhang Q C, Callanan R, Capell C, Clayton J, Donofrio M, Haney S, Husna F, Jonas C, Richmond J and Sumakeris J J 2009 *Mater. Sci. Forum* **600–603** 1183
- [6] Sugawara Y, Takayama D, Asano K, Agarwal A, Ryu S, Palmour J and Ogata S 2004 *Proceedings of 2004 International Symposium on Power Semiconductor Devices & ICs* p365
- [7] Sun G S, Liu X F, Wang L, Zhao W S, Yang T, Wu H L, Yan G G, Zhao Y M, Ning J, Zeng Y P and Li J M 2010 *Chin. Phys. B* **19** 088101
- [8] Hecht C, Stein R, Thomas B, Wehrhahn-Kilian L, Rosberg J, Kitahata H and Wischmeyer F 2010 *Mater. Sci. Forum* **645–648** 89
- [9] Sun G S, Zhao Y M, Wang L, Wang L, Zhao W S, Liu X F, Ji G and Zeng Y P 2009 *Mater. Sci. Forum* **600–603** 147
- [10] Chafai M, Jaouhari A, Torres A, Antón R, Martín E, Jiménez J and Mitchel W C 2001 *J. Appl. Phys.* **90** 5211
- [11] Harima H, Nakashima S and Uemura T 1995 *J. Appl. Phys.* **78** 1996
- [12] Yugami H, Nakashima S, Mitusishi A, Uemoto A, Shigeta M, Furukawa K, Suzuki A and Nakajima S 1987 *J. Appl. Phys.* **61** 354
- [13] Irmer G, Wenzel M and Monecke J 1997 *Phys. Rev. B* **56** 9524
- [14] Irmer G, Toporov V V, Bairamov B H and Monecke J 1983 *Phys. Status Solidi B* **119** 595
- [15] Faust W L and Henry C H 1966 *Phys. Rev. Lett.* **17** 1265
- [16] Klein M V 1975 in: Cardona M *Light Scattering in Solids* (Springer, Berlin) p147
- [17] Feldman D W, Parker Jr J H, Choyke W J and Patrick L 1968 *Phys. Rev.* **170** 698
- [18] Feldman D W, Parker Jr J H, Choyke W J and Patrick L 1968 *Phys. Rev.* **173** 787
- [19] Colwell P J and Klein M V 1972 *Phys. Rev. B* **6** 498
- [20] Sun G S, Ning J, Gong Q C, Gao X, Wang L, Liu X F, Zeng Y P and Li J M 2006 *Mater. Sci. Forum* **527–529** 191